TISSUE ENGINEERING: Part A
Volume 17, Numbers 7 and 8, 2011

DOI: 10.1089/ten.tea.2010.0070

Characteristics of High-Molecular-Weight Hyaluronic Acid as a Brain-Derived Neurotrophic Factor Scaffold in Periodontal Tissue Regeneration

Katsuhiro Takeda, D.D.S., Ph.D., Noriyuki Sakai, D.D.S., Ph.D., Hideki Shiba, D.D.S., Ph.D., Takayoshi Nagahara, D.D.S., Ph.D., Tsuyoshi Fujita, D.D.S., Ph.D., Mikihito Kajiya, D.D.S., Ph.D., Tomoyuki Iwata, D.D.S., Ph.D., Shinji Matsuda, D.D.S., Kazuko Kawahara, Ph.D., Hiroyuki Kawaguchi, D.D.S., Ph.D., and Hidemi Kurihara, D.D.S., Ph.D.

Brain-derived neurotrophic factor (BDNF), for which bovine collagen-derived atelocollagen is used as a scaffold, enhances periodontal tissue regeneration. However, a scaffold that does not contain unknown ingredients is preferable. Since the synthesized high-molecular-weight (HMW)-hyaluronic acid (HA) is safe and inexpensive, we evaluated the efficacy of HMW-HA as a BDNF scaffold. CD44, a major receptor of HA, was expressed in cultures of human periodontal ligament cells, and HMW-HA promoted the adhesion and proliferation of human periodontal ligament cells, although it did not influence the mRNA expression of bone (cementum)-related proteins. The *in vitro* release kinetics of BDNF from HMW-HA showed that BDNF release was sustained for 14 days. Subsequently, we examined the effect of BDNF/HMW-HA complex on periodontal tissue regeneration in dogs. A greater volume of newly formed alveolar bone and a longer newly formed cementum were observed in the BDNF/HMW-HA group than in the HMW-HA group, suggesting that HMW-HA assists the regenerative capacity of BDNF, although HMW-HA itself does not enhance periodontal tissue regeneration. Neither the poly (lactic-co-glycolic acid) group nor the BDNF/poly (lactic-co-glycolic acid) group enhanced periodontal tissue regeneration. In conclusion, HMW-HA is an adequate scaffold for the clinical application of BDNF.

Introduction

Brain-derived neurotrophic factor (BDNF) plays a role in the survival and differentiation of central and peripheral neurons by binding to the receptor trkB.[1–4] BDNF and its receptor trkB are also expressed in non-neural cells, such as periodontal ligament cells, cementoblasts, endothelial cells, osteoblasts, and immune cells, and regulate these cells as well as neural cells.[5–10]

The ultimate goal of periodontal treatment is complete regeneration of periodontal tissues that have been lost as a consequence of periodontal disease. Such regeneration requires the production of functional periodontal tissue composed of newly formed cementum and alveolar bone and the growth of connective tissue fibers into these hard tissues; that is, regrowth of the periodontal ligament. The formation of cementum is a key phenomenon for establishing a functional periodontium.[11] A certain fraction of periodontal ligament cells are thought to differentiate into cementoblasts or osteoblasts.[12–14] The development of a reliable biological procedure for regenerating periodontal tissue is an urgent problem, and we recently demonstrated that BDNF promotes functional periodontal tissue regeneration by regulating the function of periodontal ligament cells, endothelial cells, and cementoblasts.[5–7] However, bovine atelocollagen sponge has also been used as a scaffold for BDNF.[5] Atelocollagen is purified from bovine dermal type I collagen, and it may contain unknown proteins. Thus, we consider that a scaffold consisting of only known ingredients is preferable. Therefore, we attempted to find an alternative scaffold for the clinical application of BDNF. It is important that the scaffold maintains the activity of BDNF and is safe, inexpensive, biodegradable, biocompatible, and space maintaining. A large array of biomaterials, such as autogenous bone grafts, bone allografts, tricalcium phosphate ceramics, hydroxyapatite, polylactic acid, polyglycolic acid, copolymers of polylactic acid and polyglycolic

This work was performed at the Division of Frontier Medical Science, Department of Periodontal Medicine, Hiroshima University Graduate School of Biomedical Sciences, Hiroshima, Japan.
Division of Frontier Medical Science, Department of Periodontal Medicine, Hiroshima University Graduate School of Biomedical Sciences, Hiroshima, Japan.

acid, bioactive glasses, and biocomposites, have been proposed as ideal scaffolds for tissue regeneration.[15] However, few scaffolds have demonstrated clinical efficacy.

Hyaluronic acid (HA) is a nonsulfated, linear glycosaminoglycan consisting of repeating units of (β, 1–4) glucuronic acid–(β, 1–3)-N-acetyl glucosamine. Besides its function in the viscoelasticity of joint synovial fluid and the organization of the cartilage extracellular matrix,[16] HA plays a crucial role in wound healing.[17–20] HA is present in most living tissues as a high-molecular-mass polymer ($>10^6$ Da) and in significant quantities in the skin (dermis and epidermis), brain, and central nervous system.[21] In addition, HA fragments of low molecular mass ($<10^6$ Da) are produced as a result of hyaluronidases or oxidation after tissue injury.[22] High-molecular-weight (HMW)-HA and low-molecular-weight (LMW)-HA exert various mitogenic effects, depending on the cell type and source in addition to the concentration of HA.[23] Compared to LMW-HA, HMW-HA has following properties: a longer residence time, higher viscosity, and higher biocompatibility.[24] HMW-HA also has anti-inflammatory effects. HMW-HA inhibits mRNA expression of interleukin (IL)-1β, IL-6, and tumor necrosis factor-α, and cyclooxygenase-2/prostaglandin E_2 production in IL-1-stimulated synovial fibroblasts.[25] However, the mechanism of the different action between LMW-HA and HMW-HA is not fully understood.

We proposed that synthesized HMW-HA would be a suitable scaffold for BDNF since HMW-HA has appropriate properties for a scaffold. In the present study, we examined the effects of HMW-HA on the adhesion, proliferation, and expression of bone (cementum)-related proteins in cultures of human periodontal ligament (HPL) cells to elucidate the *in vitro* potential of HMW-HA as a delivery vehicle for BDNF. Further, we evaluated the effect of BDNF/HMW-HA complex on periodontal tissue regeneration in inflamed class III furcation defects in beagles.

Materials and Methods

BDNF and synthesized HMW-HA

Recombinant human BDNF was supplied from Dainihon Sumitomo Pharmaceutical Co., Ltd. It was diluted with 10 mM sodium phosphate and 150 mM NaCl (pH 7.0). The synthesized HMW-HA, the molecular weight of which was 2 million, was supplied from DENKA Co., Ltd.

Cell culture

Two HPL cell lines (HPL cells-1 and HPL cells-2) were separately obtained from explant cultures of healthy periodontal ligaments of the midroots of premolars extracted from two patients under orthodontic treatment with their informed consent. Informed consent was obtained under a protocol approved by the ethics authorities at Hiroshima University. The periodontal ligament tissue was cut into small pieces and plated in a 35-mm-diameter plastic culture dish with Dulbecco's modified Eagle's medium (DMEM) supplemented with 10% fetal bovine serum (FBS; GIBCO), which is used to enhance HPL cell growth, 100 units/mL penicillin, 100 μg/mL streptomycin, and 1 μg/mL amphotericin B (medium A). When the HPL cells had formed a confluent monolayer, the cells were harvested with 0.05% trypsin and 0.02% ethylenediaminetetraacetic acid and then transferred to a 100-mm-diameter plastic culture dish. Sixth-passage HPL cells were used in the following experiments.

Immunofluorescence microscopy

HPL cells were cultured until subconfluence on 35-mm Glass Base Dishes® (IWAKI), washed with phosphate-buffered saline (PBS), and fixed with 4% paraformaldehyde in PBS for 10 min. Nonspecific binding was blocked by incubation with Tris buffered saline (TBS) containing 0.2% casein and 0.1% Triton X-100 for 20 min. The cells were then incubated with mouse anti-human CD44 monoclonal antibody (Ancell, 1:200) at 4°C overnight. After being washed three times with PBS for 5 min, the cells were incubated with secondary Alexa Fluor® 488 anti-mouse IgG (Life Technologies, 1:200) for 1 h at room temperature. 4′,6-Diamino-2-phenylindole (DAPI) was stained with anti-Fade DAPI Fluoromount$^+$-G (Southern Biotech). After rinsing the cells with PBS, fluorescence signals were detected with a Zeiss LSM 510 laser scanning confocal microscope (Zeiss Microimaging, Inc.).

Flow cytometry analysis

HPL cells were harvested with Cell Dissociation buffer Enzyme-Free PBS-based from Invitrogen and incubated with mouse anti-human CD44 monoclonal antibody (1:200) (Ancell) for 30 min. After incubation with the primary antibody, the cells were fixed with 1% paraformaldehyde and rinsed with 1 M sodium phosphate buffer. Then, the cells were incubated with horse anti-mouse IgG-FITC (Vector Laboratories) for 30 min. Mouse IgG1 K Isotype Control (ebioscience) was used as a negative control. Next, the cells were subjected to flow cytometry analysis using a BD FACS Calibur (Becton Dickinson). The cells were gated according to their high fluorescence intensity.

Cell adhesion assay

Ninety-six-well plates were precoated with 100 μL of HMW-HA for 24 h at 4°C. The wells were washed three times with PBS, and nonspecific binding was blocked with 2% bovine serum albumin (BSA) for 30 min before the addition of the cells at 2×10^4/well in DMEM. The wells that had not been precoated with HMW-HA were treated with 2% BSA as a control. The cells were then incubated in the presence or absence of mouse anti-human CD44 antibody (5 μg/mL; Ancell) for 2 h at 37°C. Nonadherent cells were removed by washing three times with DMEM. The remaining adherent cells were fixed in 1% glutaraldehyde for 15 min and stained with 0.1% crystal violet. The stain was eluted from the remaining adherent cells with 10% acetic acid, and the absorbance was read at 600 nm.

DNA synthesis

DNA synthesis was estimated by measuring the incorporation of bromodeoxyuridine (BrdU) using a cell proliferation ELISA system (Version 2; Amershampharmacia). HPL cells in cultures of the sixth passage were harvested, seeded at a density of 5×10^3 cells/6 mm in plastic tissue culture dishes, and maintained in 0.1 mL of medium A supplemented with 50 μg/mL ascorbic acid (medium B). After 12 days, these cells were washed three times with DMEM and incubated in

DMEM supplemented with 100 units/mL penicillin, 100 μg/mL streptomycin, 1 μg/mL amphotericin B, and 50 μg/mL ascorbic acid (medium C) supplemented with 0.3% FBS for 24 h. The cells were then incubated with various concentrations of HMW-HA in fresh medium C together with 0.3% FBS for 24 h. BrdU (10 ng/mL) was added 3 h before the end of incubation. Immunodetection of the BrdU incorporated into the cells was performed according to the manufacturer's instructions.

Isolation of total RNA and reverse transcription

HPL cells in cultures of the sixth passage were harvested, seeded at a density of 3.5×10^5 cells/60 mm in plastic tissue culture dishes, and maintained in medium B. The HPL cells were then exposed to various concentrations of HMW-HA for the indicated times before the end of incubation on day 14 in medium C. Total RNA from each culture was extracted using ISOGEN® (Wako Pure Chemical Industries) on day 14 and quantified by spectrometry at 260 and 280 nm. Two micrograms from each total RNA extract were used to perform first-strand cDNA synthesis with a first-strand cDNA synthesis kit (Roche) in a total volume of 20 μL. Then, one-tenth of each generated cDNA was used as template DNA for real-time polymerase chain reaction (PCR).

Real-time PCR

The mRNA expression levels of alkaline phosphatase (ALP), osteopontin (OPN), osteocalcin (OCN), and bone morphogenetic protein (BMP)-2 were quantified by real-time PCR. The PCR was carried out in two steps with a Light-cycler system using SYBR Green (Roche Diagnostics). The sense primers and antisense primers were as follows—ALP: 5′-GCGGTGAACGAGAGAATG-3′, 5′-CGTAGTTCTGCTC GTGGAC-3′; OPN: 5′-GATGGCCGAGGTGATAGTGT-3′, 5′-CCATTCAACTCCTCGCTTTC-3′; OCN: 5′-GCAGCGAGG TAGTGAAGAGAC-3′, 5′-GGTCAGCCAACTCGTCACAG-3′; BMP-2: 5′-CTGTATCGCAGGCACTCA-3′, 5′-CTCCGTG GGGATAGAACTT-3′; GAPDH: 5′-AACGTGTCAGTGGTG GACCTG-3′, 5′-AGTGGGTGTCGCTGTTGAAGT-3′.

In vitro *release kinetics of BDNF*

The BDNF released from HMW-HA was measured using a sandwich enzyme-linked immunosorbent assay. A Transwell® Insert with an 8.0 μm pore membrane (CORNING) was placed in a six-well plastic culture plate. The upper and lower wells contained 5 μg of BDNF in 1 mL HMW-HA and 2 mL of PBS, respectively. The plate with the Transwell Insert was incubated at 37°C and 5% CO_2 during the experiment. The PBS in the lower well was replaced every day with 2 mL of fresh PBS for up to 14 days. The PBS samples from the lower well were collected and then preserved at −20°C until analysis. The BDNF concentrations of the samples were determined using a sandwich ELISA kit for BDNF (R&D Systems).

Experimental model for periodontal tissue regeneration

After having obtained the approval of the Committee of Research Facilities for Laboratory Animal Science of Hiroshima University School of Medicine, 10 female beagles (2 weeks observation model: 1 dog; 6 weeks observation model: 9 dogs) weighing 10–14 kg and aged 12–20 months were used in the present study. Their good oral health was ensured by scaling and mechanical tooth brushing.

Creation of class III furcation defects and transplantation of BDNF/HMW-HA complex

All surgical procedures were performed under general anesthesia induced with Nembutal® (40 mg/kg; Abbott Laboratories) and local anesthesia induced with Xylocaine® (2% lidocaine with 1:80,000 noradrenaline; Fujisawa). The mandibular second, third, and fourth premolars (P2, P3, and P4) on the right and left sides from 10 beagle dogs were used for the following experiment. After sulcular incisions had been made, full-thickness flaps were raised, and class III furcation defects were surgically created (Fig. 1A) with the use of bone chisels and slowly rotating round burs. Sterile saline was used to irrigate the soft and hard tissues during the surgical procedure. The defect height from the cement–enamel junction to the reduced alveolar crest was 4 mm. The exposed periodontal ligaments and cementum were completely removed to produce denuded root surfaces. Reference notches were placed on the mesial and distal roots to indicate the bottom of the defect. Then, the defects were filled with alginate impression material (MORITA) to induce inflammation (Fig. 1B). The flaps were then replaced to their original position and sutured with interdental sutures.

One week after the impression material had been inserted, it was surgically removed. During the next week, all test and control sites were mechanically cleaned by supra- and subgingival scaling and root planing for the prevention of plaque accumulation and periodontal inflammation.

One week after the removal of the alginate impression material, the reconstructive procedure was carried out. BDNF at concentrations of 5, 50, 500, and 2000 μg/mL was prepared by diluting it with HMW-HA (Fig. 1C). After careful scaling and root planing, BDNF/HMW-HA complex was applied into the defects (Fig. 1D). The flaps were then coronally repositioned and sutured by the interrupted suture method with 4-0 silk sutures. During the subsequent 2 or 6 weeks, good oral hygiene was maintained by brushing and swabbing with 0.2% povidone iodine solution (Meiji-seika Co., Ltd.). We compared the periodontal tissue regeneration in the BDNF/HMW-HA group with that in the HMW-HA alone application group and the sham operation group, which contains neither BDNF nor HMW-HA. We also compared the periodontal tissue regeneration in the BDNF/HMW-HA group with that in the BDNF (50 μg/mL)/poly (lactic-co-glycolic acid) (PLGA) (GC) group to examine the effectiveness of HMW-HA as a scaffold of BDNF.

Tissue preparation for histological analysis

After the surgery, the anesthetized animals were perfused with 4% paraformaldehyde in 0.1 M sodium phosphate buffer (pH 7.2). Their mandibles were then dissected and immersed in the same fixative. After decalcification with KCX® (FALMA Co., Ltd.) and 10% ethylenediaminetetraacetic acid (NACALAI TESQUE) for 2 and 8 weeks, respectively, the tissues were dehydrated through graded ethanol, cleared with xylene, and embedded in paraffin. Serial sections (5 μm) were cut in the mesial-distal plane throughout the buccal-lingul extension of the teeth. The sections showing the center of the furcation site

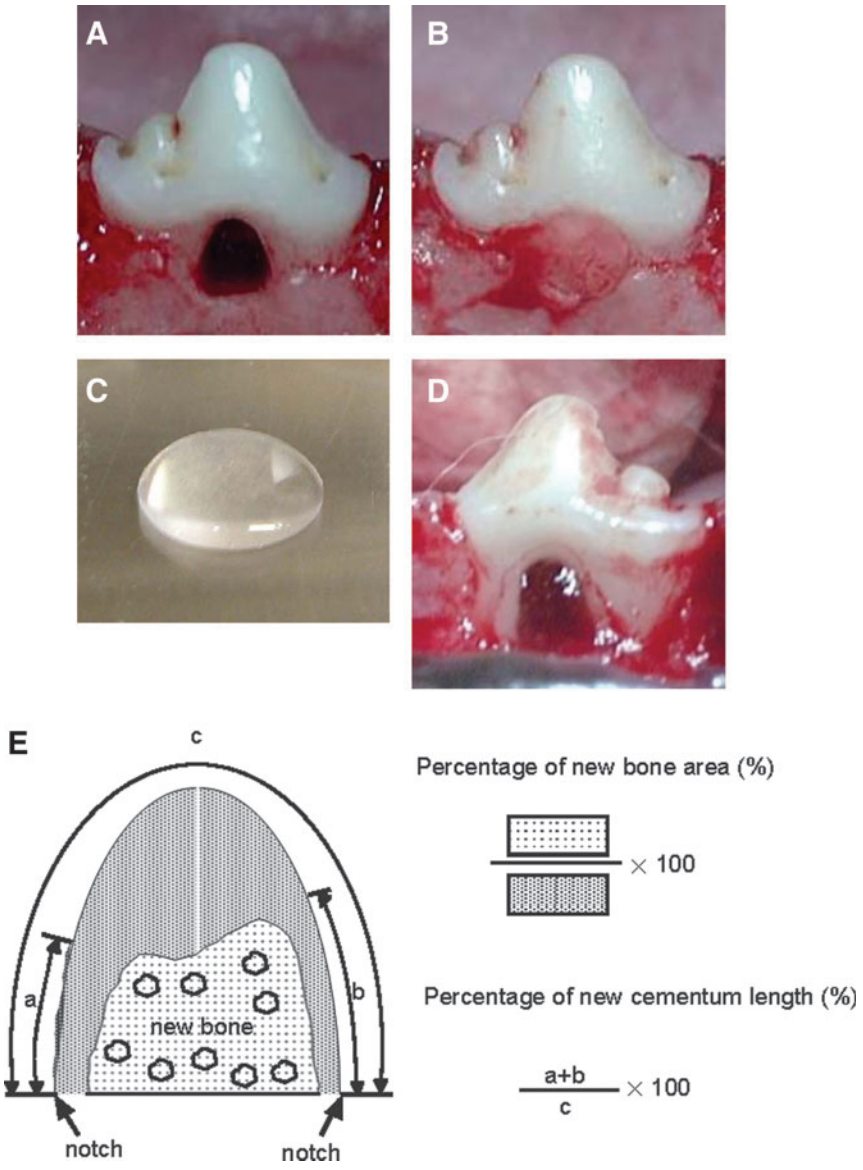

FIG. 1. Creation of inflamed class III furcation defects and the application of brain-derived neurotrophic factor (BDNF). **(A)** Defect preparation; **(B)** inserting the alginate impression material to induce inflammation; **(C)** synthesized high-molecular-weight-hyaluronic acid (HMW-HA); **(D)** application of BDNF/HMW-HA complex; **(E)** schematic drawing of the histometric analysis of percentages of the new bone area and cementum length.

were then stained with hematoxylin and eosin (HE) and observed using a light microscope.

Morphometrical analysis

Since 6 premolars were not available because of technical failure, 48 teeth from 9 dogs were used for the analysis of eight groups (sham operation, HMW-HA alone, 5 μg/mL BDNF+HMW-HA, 50 μg/mL BDNF+HMW-HA, 500 μg/mL BDNF+HMW-HA, 2000 μg/mL BDNF+HMW-HA, PLGA alone, and 50 μg/mL BDNF/PLGA). The length of newly formed cementum and the area of newly formed bone were measured using the software NIH Image® on digitized photomicrographs captured by a Windows® computer. New cementum formation was represented as the percentage of new cementum length formed along the denuded root surface to the total root surface length from notch to notch (Fig. 1E). The area of newly formed bone on each specimen was calculated as the percentage of the area surrounded by reference notches on the mesial and distal root surfaces facing the bone defect (Fig. 1E). Since the periodontal ligament space is present in normal periodontal tissue, the percentage of bone area in normal specimens was 83%.

Azan staining

Some sections were stained using the Azan method[5] to observe collagen fibers. The deparaffinized and hydrated sections were immersed in azocarmine G solution for 30 min at 56°C–60°C, rinsed with aniline alcohol solution and 1% acetic acid in ethanol, soaked in 5.0% phosphotungstic acid aqueous solution for 60 min at room temperature, and dipped in aniline blue-orange G solution for 30 min at room temperature.

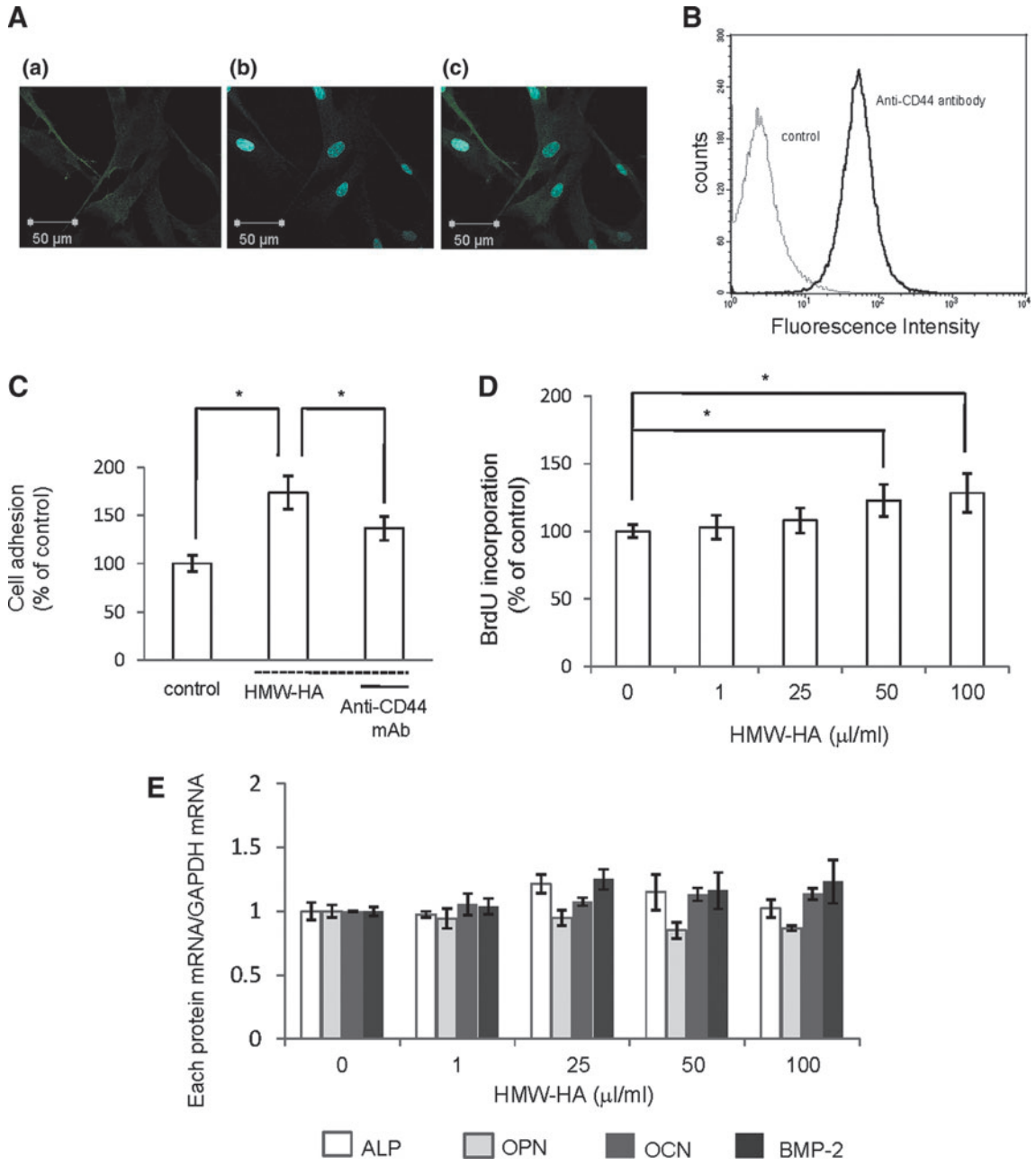

FIG. 2. **(A)** CD44 expression in human periodontal ligament (HPL) cells-1. Fluorescence signals were detected with a laser scanning confocal microscope. **(a)** CD44, **(b)** 4′, 6-diamino-2-phenylindole, and **(c)** merging of **(a)** and **(b)**. Bars: 50 μm. **(B)** Flow cytometry analysis of surface CD44 expression in HPL cells-1. HPL cells-1 were stained with antibodies against CD44 or the control antibody and subjected to flow cytometry analysis. The black line represents CD44 staining, and the gray line represents staining with the control antibody. **(C)** HPL cells-1 adhesion to HMW-HA. HPL cells-1 were seeded in bovine serum albumin-coated wells as a control and in HMW-HA-coated wells in the presence or absence of mouse anti-human CD44 antibody (5 μg/mL). The cells were allowed to adhere for 2 h at 37°C. After the incubation, the adherent cells were stained with crystal violet. The stain was then eluted from the cells with acetic acid, and the absorbance was read at 600 nm. Values represent the mean ± standard deviation (SD) of three cultures. $*p < 0.01$: differs significantly from the control. **(D)** DNA synthesis in HPL cells-1. HPL cells-1 were exposed to various concentrations of HMW-HA for 24 h before the end of incubation on day 12. DNA synthesis was estimated by measuring the incorporation of bromodeoxyuridine (BrdU). Values represent the mean ± SD of three cultures. $*p < 0.01$, differs significantly from the control. **(E)** Effects of HMW-HA on osteopontin (OPN), bone morphogenetic protein 2 (BMP-2), alkaline phosphatase (ALP), and osteocalcin (OCN) mRNA expression in HPL cells-1. HPL cells-1 were exposed to various concentrations of HMW-HA for 24 h before the end of incubation on day 14. The mRNA expression of OPN, BMP-2, ALP, and OCN was determined by real-time polymerase chain reaction. The graph shows the ratios of OPN, BMP-2, ALP, and OCN mRNA to GAPDH mRNA. Values represent the mean ± SD of three cultures.

Immunohistochemical procedures

The sections were deparaffined with xylene, rehydrated through a descending ethanol series, and washed in distilled water, before being treated with 0.1% trypsin for 15 min at 37°C and rinsed in distilled water. Endogenous peroxidase was blocked by incubating the sections with 3% hydrogen peroxide for 10 min. After washing the sections with TBS (pH 7.2), they were treated with 0.1% BSA (Sigma) for 10 min at 37°C to prevent nonspecific binding. Then, the sections were incubated for 1 h at room temperature with rat anti-human CD44 monoclonal antibody (1:250) (Millipore Corporation), goat anti-mouse OPN monoclonal antibody (1:50) (COSMO BIO USA Inc.), and rabbit anti-human protein gene protein (PGP) 9.5 polyclonal antibody (1:400) (Abcam Inc.), diluted with DAKO antibody diluent (DAKO Corporation). After incubation with the primary antibodies, the sections were rinsed and incubated with TBS for 30 min at room temperature in a moist chamber. Then, the sections were incubated with biotinylated goat anti-rabbit IgG (1:200; Vector Laboratories), donkey anti-goat IgG (1:200; Vector Laboratories), or goat anti-rat IgG antibody (1:2000; Invitrogen) for 30 min in a moist chamber, rinsed with TBS, and incubated with streptavidin peroxidase conjugate (DAKO LSAB kit; DAKO Corporation) for 15 min. Finally, the sections were rinsed in TBS. Antibody complexes were observed with 3, 3′-diaminobenzidine substrate, washed in distilled water, and counterstained with hematoxylin.

Results

Immunofluorescence showed that CD44 was expressed in the HPL cells-1 [Fig. 2A (a)], and DAPI-stained HPL cells-1 nuclei were also observed [Fig. 2A (b)]. From the merging of Figure 2A (a) and 2A (b), CD44 proteins were localized in the cytoplasm of the HPL cells-1 [Fig. 2A (c)]. Flow cytometry analysis also showed that the HPL cells-1 were positive for CD44 expression (Fig. 2B). HPL cells-1 adhesion to HMW-HA-coated plates was significantly promoted in comparison with that seen in BSA-coated plates (control) (Fig. 2C). The number of HPL cells-1 attached to the HMW-HA-coated plates was increased 1.73-fold compared to that of the control. The adhesion of HPL cells-1 was significantly inhibited by anti-CD44 neutralizing antibody (Fig. 2C). HMW-HA at 50 and 100 μL/mL significantly increased BrdU incorporation in the HPL cells-1 (Fig. 2D). The dose–course experiments showed that HMW-HA did not influence bone (cementum)-related protein mRNA expression in the HPL cells-1 (Fig. 2E). The results of each *in vitro* experiment using HPL cells-2 were similar to those of the same experiment using HPL cells-1 (data not shown).

The concentration of BDNF released from HMW-HA increased in a time-dependent manner until the third day, and the maximal concentration of BDNF was 143.1 ± 28.7 ng/mL (Fig. 3). Then, the release of BDNF decreased steeply to 61.1 ± 11.5 ng/mL until the fifth day, before sustained release of BDNF of around 60 ng/mL was observed until day 13. The release of BDNF had decreased to 16.8 ± 3.6 ng/mL by day 14. A total of 1.01 μg (20% of the initial BDNF loaded) was found to be released from HMW-HA during the study.

Two weeks after the surgery, no epithelial cell invasion into the top of the furcation area was observed in the HMW-HA/BDNF group (Fig. 4A). However, alveolar bone regeneration was insufficient at this time. CD44-immunoreactive cells were present in the healthy periodontal ligament (Fig. 4B), and CD44-immunoreactive cells were observed in the connective tissue of the defect (Fig. 4C) as well as on the dentin surface (Fig. 4D).

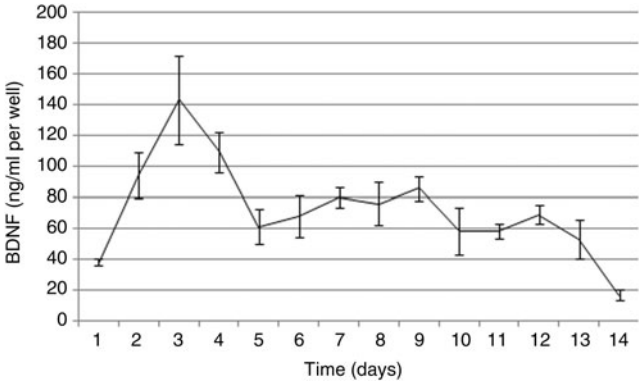

FIG. 3. Release kinetics of BDNF from HMW-HA. Line chart showing noncumulative release at each time point. The protein level of BDNF was assayed using an ELISA kit. Values represent the mean ± SD of five cultures.

Six weeks after the surgery, epithelial cells invaded the top of the furcation in the sham operation group, which contain neither HMW-HA nor BDNF, and HMW-HA groups (Fig. 5A, B). Less inflammatory cell infiltration was observed in the HMW-HA group than in the sham operation group (Fig. 5A, B). The HMW-HA group seemed to show enhanced periodontal tissue regeneration slightly compared to the sham operation group according to HE staining (Fig. 5A, B). Morphometrical analyses of the new bone area showed that the percentages of new bone area in the sham operation and HMW-HA alone groups were 5.2 ± 5.2 and 34.7 ± 23.1, respectively (Fig. 6A). The percentages of new cementum length in the sham operation and HMW-HA alone groups were 19.0 ± 7.8 and 37.0 ± 26.7, respectively (Fig. 6B). No statistically significant difference in the new bone area or new cementum length was observed between the HMW-HA group and the sham operation group (Fig. 6A, B). The BDNF/HMW-HA group showed enhanced periodontal tissue regeneration without epithelial cell invasion into the top of the furcation area (Fig. 5C). No marked inflammatory cell infiltration was observed in the BDNF/HMW-HA or HMW-HA group (Fig. 5B, C). Morphometrical analyses of new bone area showed that the percentages of new bone area in the 5, 50, 500, and 2000 μg/mL BDNF+HMW-HA groups were 58.0 ± 19.0, 67.7 ± 12.5, 56.1 ± 15.4, and 64.2 ± 5.3, respectively (Fig. 6A). BDNF at 50 and 2000 μg/mL significantly increased bone area compared to the HMW-HA group (Fig. 6A). Further, the percentages of new cementum length in the 5, 50, 500, and 2000 μg/mL BDNF+HMW-HA groups were 75.1 ± 16.5, 89.6 ± 18.3, 77.8 ± 10.1, and 79.8 ± 12.4, respectively (Fig. 6B). BDNF at 5, 50, and 2000 μg/mL significantly increased cementum length compared to the HMW-HA group (Fig. 6B).

Secondary, we compared the effectiveness of HMW-HA as a BDNF scaffold with that of PLGA. Six weeks after the surgery, epithelial cells invaded the top of the furcation in the PLGA groups as well as the HMW-HA groups (Fig. 5B, E). Less inflammatory cell infiltration was observed in the

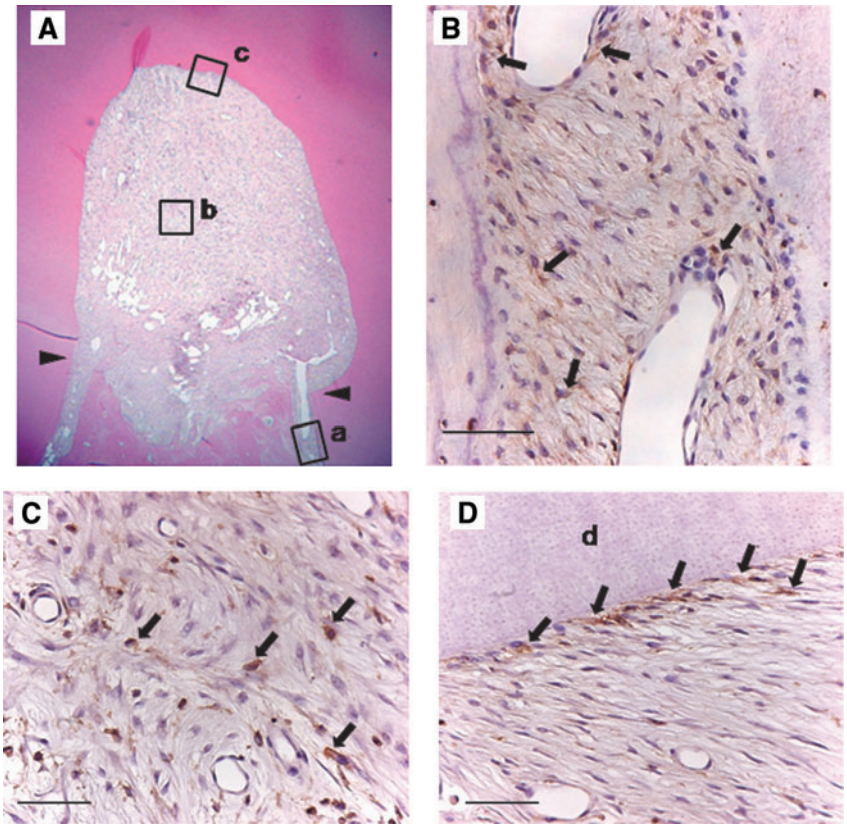

FIG. 4. Immunolocalization of CD44 during the early phase of the regeneration of experimentally created periodontal defects in the BDNF (50 μg/mL)/HMW-HA group. **(A)** Low-power view of the furcation representing BDNF (50 μg/mL)/HMW-HA group 2 weeks after the application of the treatments. The tissues were decalcified with 10% ethylenediaminetetraacetic acid for 8 weeks. Arrowheads: apical borders of the notches. Hematoxylin and eosin (HE) staining. Original magnification: ×20. **(B)** Magnification of the rectangular area shown in **A**(a). Arrows: CD44-immunoreactive cells. Bar: 20 μm. **(C)** Magnification of the rectangular area shown in **A**(b). Arrows: CD44-immunoreactive cells. Bar: 20 μm. **(D)** Magnification of the rectangular area shown in **A**(c). Arrows: CD44-immunoreactive cells. d, dentin. Bar: 20 μm.

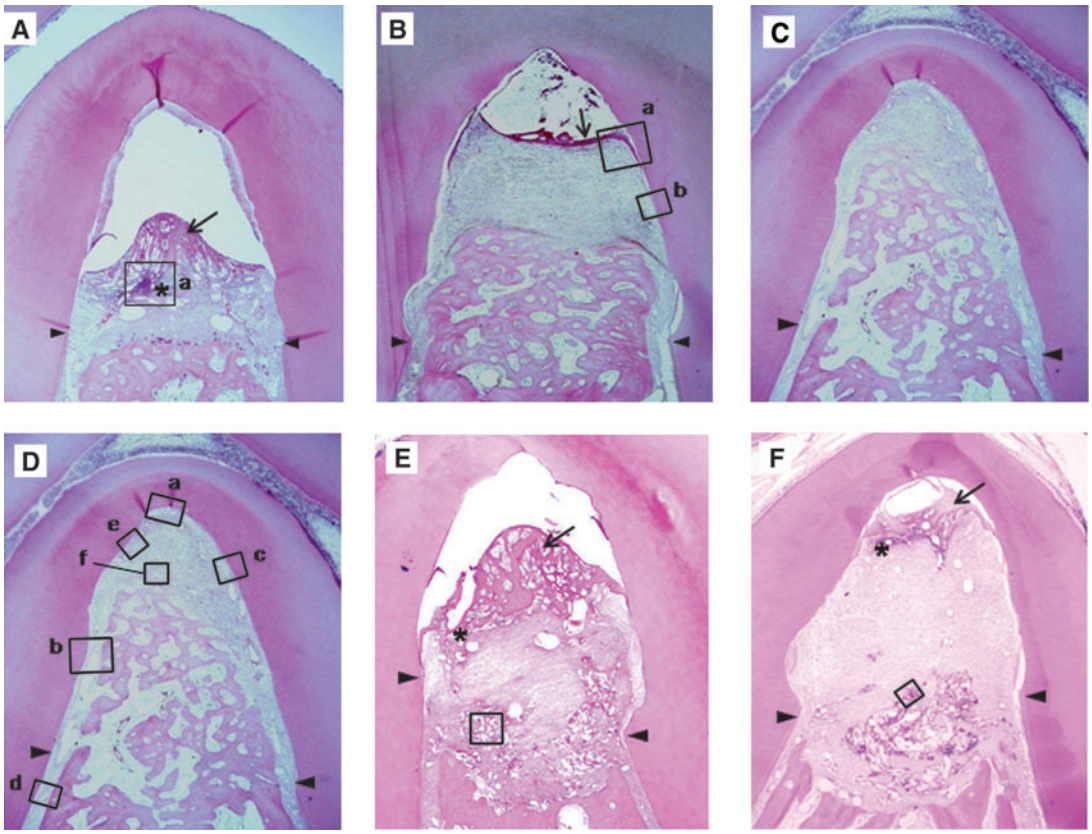

FIG. 5. Effect of BDNF/HMW-HA complex in experimentally created periodontal defects. The photographs are low-power views of furcations representing the sham operation **(A)**, HMW-HA group **(B)**, BDNF (50 μg/mL)/HMW-HA group **(C, D)**, poly (lactic-co-glycolic acid) (PLGA) group **(E)**, and BDNF (50 μg/mL)/PLGA group **(F)** 6 weeks after the application of the treatments. Arrows: epithelial cell invasion. Arrowheads: apical borders of the notches. Boxed areas are shown magnified in Figures 7, 8 and 9. *Inflammatory cell infiltration. HE staining. Original magnification: ×20.

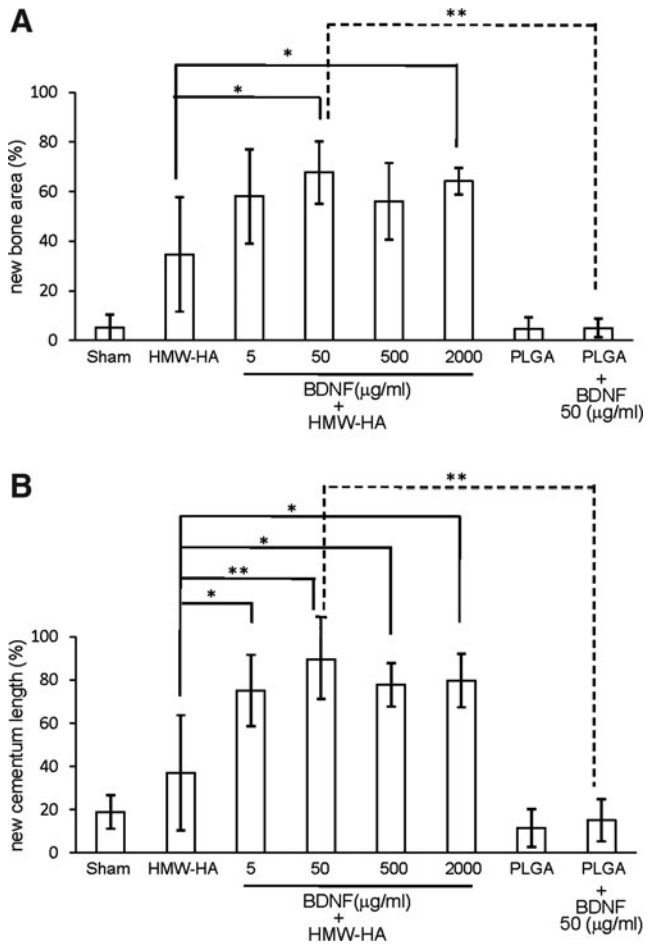

FIG. 6. Morphometrical analysis of the effect of BDNF/HMW-HA complex. The graphs show the percentages of new bone area **(A)** and new cementum length **(B)** according to morphometrical analysis. Seven teeth from nine dogs were used for the HMW-HA group and each BDNF/HMA-HA complex group. Three teeth from nine dogs were used for the sham operation. Five teeth from nine dogs were used for the PLGA group and the BDNF (50 μg/mL)/PLGA group. The tissues were decalcified with KCX (FALMA Co., Ltd) for 2 weeks. Three sections per tooth were examined for morphometrical analysis. The results of the HMW-HA group and the BDNF/HMW-HA groups are expressed as the mean ± SD of 21 sections for each group. The result of the sham operation group is expressed as the mean ± SD of nine sections. The results of the PLGA group and the BDNF (50 μg/mL)/PLGA group are expressed as the mean ± SD of 15 sections for each group. $*p < 0.05$, $**p < 0.01$: differs significantly from the control.

HMW-HA group than in the PLGA group (Fig. 5B, E). The HMW-HA group seemed to show enhanced periodontal tissue regeneration slightly compared to the PLGA group according to HE staining (Fig. 5B, E). Morphometrical analyses of the new bone area showed that the percentages of new bone area in the PLGA group and HMW-HA alone groups were 4.7 ± 4.6 and 34.7 ± 23.1, respectively (Fig. 6A). The percentages of new cementum length in the PLGA group and HMW-HA alone groups were 11.6 ± 8.8 and 37.0 ± 26.7, respectively (Fig. 6B). No statistically significant difference in the new bone area or new cementum length was observed between the PLGA group and the HMW-HA group (Fig. 6A, B). In contrast to the BDNF/HMW-HA group, the BDNF/PLGA group did not show enhanced periodontal tissue regeneration (Fig. 5F). Epithelial cell invasion into the top of the furcation and inflammatory cell infiltration were observed in the BDNF/PLGA group (Fig. 5F). Morphometrical analyses of new bone area showed that the percentages of new bone area in the BDNF (50 μg/mL)/PLGA group and in the BDNF (50 μg/mL)/HMW-HA group were 5.1 ± 3.8 and 67.7 ± 12.5, respectively (Fig. 6A). Further, the percentages of new cementum length in the BDNF (50 μg/mL)/PLGA group and in the BDNF (50 μg/mL)/HMW-HA group were 15.1 ± 9.7 and 89.6 ± 18.3, respectively (Fig. 6B).

In the sham operation group, marked inflammatory cell infiltration was observed in the connective tissue of the defect (Fig. 7A). In the HMW-HA group, epithelial cells invaded the top of the furcation, and no newly formed cementum was observed in this area (Fig. 7B). On the other hand, newly formed cementum was observed on the denuded root surfaces of the furcation area in the BDNF/HMW-HA group (Fig. 7C). The new connective tissue fibers inserted into the newly formed cementum were stained with Azan (Fig. 7D). Large blood capillaries were observed in the BDNF/HMW-HA group than in the HMW-HA group (Fig. 7B, C). The insertion of new connective tissue fibers into the bone and cementum was observed by Azan staining, suggesting that the periodontal ligament had been regenerated (Fig. 7E). Further, no epithelial cell invasion or bone ankylosis were observed at the BDNF/HMW-HA sites (Fig. 7C–E). In both the PLGA group and the BDNF (50 μg/mL)/PLGA group, marked inflammatory cell infiltration and PLGA residuals were observed in the connective tissue of the defect (Fig. 7F, G).

In the HMW-HA group, immunohistochemical analysis showed that OPN was localized at the dentine surface, but no new cementum was formed (Fig. 8A). In the BDNF/HMW-HA group, OPN showed a positive reaction at the dentin surfaces on which the cementum had regenerated (Fig. 8B). The cementoblasts lining the cementum surface were also immunoreactive for OPN (Fig. 8B).

PGP 9.5-immunoreactive cells were present in the healthy periodontal ligament (Fig. 9A), and PGP 9.5-immunoreactive cells were also observed near the dentin surface (Fig. 9B) and regenerating alveolar bone (Fig. 9C). As a negative control, an immunoglobulin fraction (DAKO) was applied instead of the primary antibody. Negative control staining showed no labeling (data not shown).

Discussion

CD44, a ubiquitously distributed transmembrane adhesion receptor, is a major receptor for HA.[26,27] CD44–HA interactions are implicated in cell migration and adhesion in addition to inflammation and tumorigenesis.[28–30] In the present study, HPL cells were found to express CD44, suggesting that the interaction between CD44 and HMW-HA regulates the function of HPL cells.

HA has been demonstrated to have properties beneficial for the promotion of tissue regeneration.[16–18] In this study, we first focused on cell adhesion and proliferation, which are the early processes of tissue regeneration before differentiation and tissue maturation.[31] It is reported that HA supports the

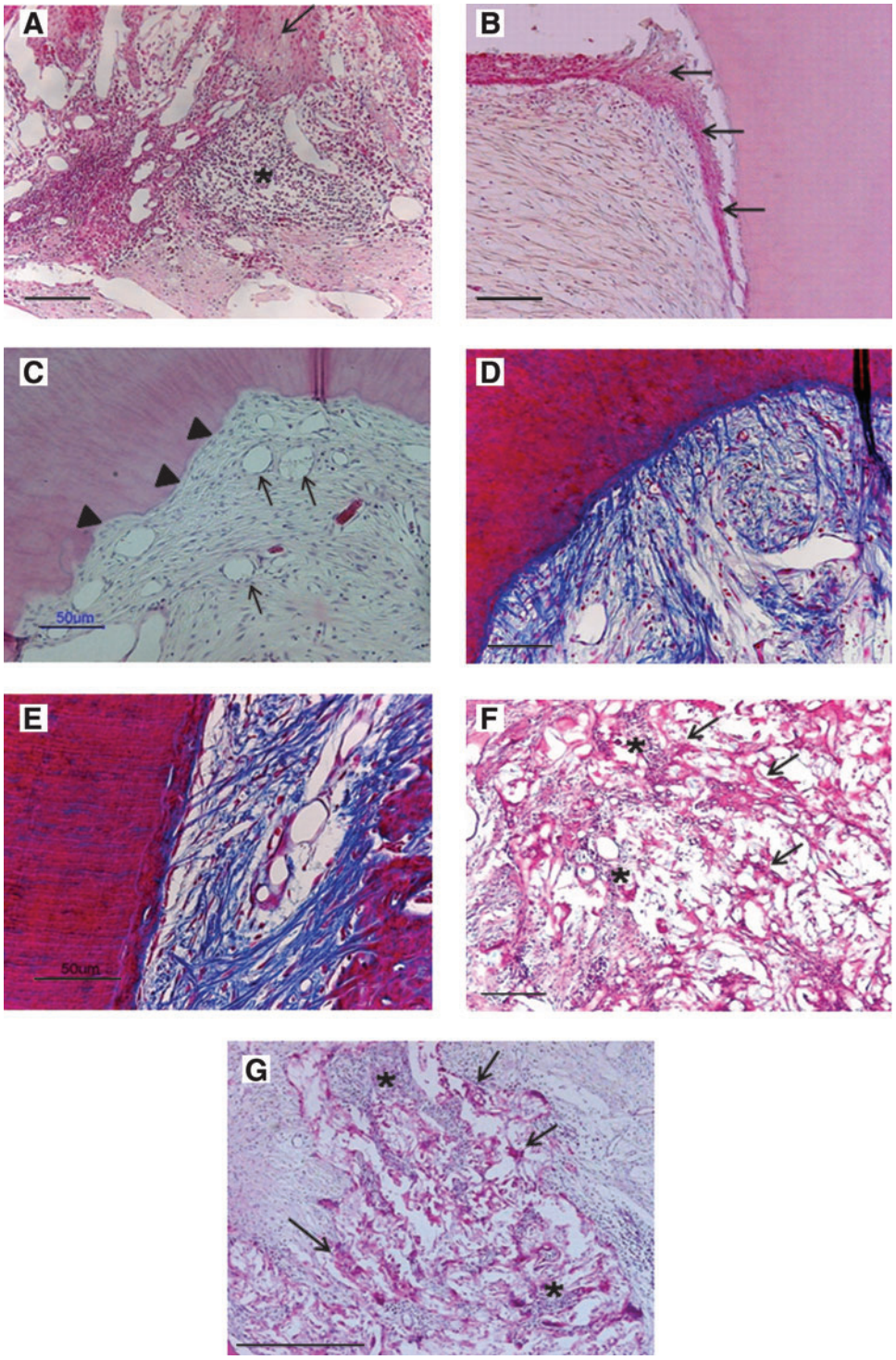

FIG. 7. Higher magnifications of Figure 5. **(A)** Magnification of the rectangular area shown in Figure 5A(a). Arrow: epithelial cell invasion. *Inflammatory cell infiltration. HE staining. Bar: 50 μm. **(B)** Magnification of the rectangular area shown in Figure 5B(a). Arrows: epithelial cell invasion. HE staining. Bar: 50 μm. **(C)** Magnification of the rectangular area in the upper area of the furcation shown in Figure 5D(a). Arrowheads: newly formed cementum. Arrows: large blood vessels. HE staining. Bar: 50 μm. **(D)** Azan staining of **(C)**. Bar: 50 μm. **(E)** Magnification of the rectangular area shown in the lower position in Figure 5D(b). Connective tissue was observed between newly formed cementum and bone. Azan staining. Bar: 50 μm. **(F)** Magnification of the rectangular area in Figure 5E. Arrows: PLGA residuals. *Inflammatory cell infiltration. HE staining. Bar: 50 μm. **(G)** Magnification of the rectangular area in Figure 5F. Arrows: PLGA residuals. *Inflammatory cell infiltration. HE staining. Bar: 50 μm.

adhesion of rat mesenchymal stem cells under static culture conditions without any chemical induction.[32] Native HA inhibits the proliferation of endothelial cells, whereas 3–10 disaccharide HA fragments stimulate their proliferation.[33] HMW-HA decreases the cell proliferation of fetal rabbit and embryogenic chick skin fibroblasts,[34,35] whereas it had a stimulatory effect on the proliferation of human dermal and NIH 3T3 fibroblasts.[36,37] The present study showed that HMW-HA increased the number of adherent HPL cells and slightly stimulated the proliferation of HPL cells. These findings suggest that HMW-HA plays a role in the early phases of periodontal tissue regeneration through CD44. The properties of HMW-HA are thought to be advantageous for the regeneration of periodontal tissue by BDNF.

Our previous studies have shown that BDNF stimulates the expression of bone (cementum)-related proteins in HPL cells and human cementoblast-like cells.[5,6] In the present study, HMW-HA did not affect their expression in HPL cells. Therefore, HMW-HA may not affect cell differentiation in the late stage of tissue regeneration.

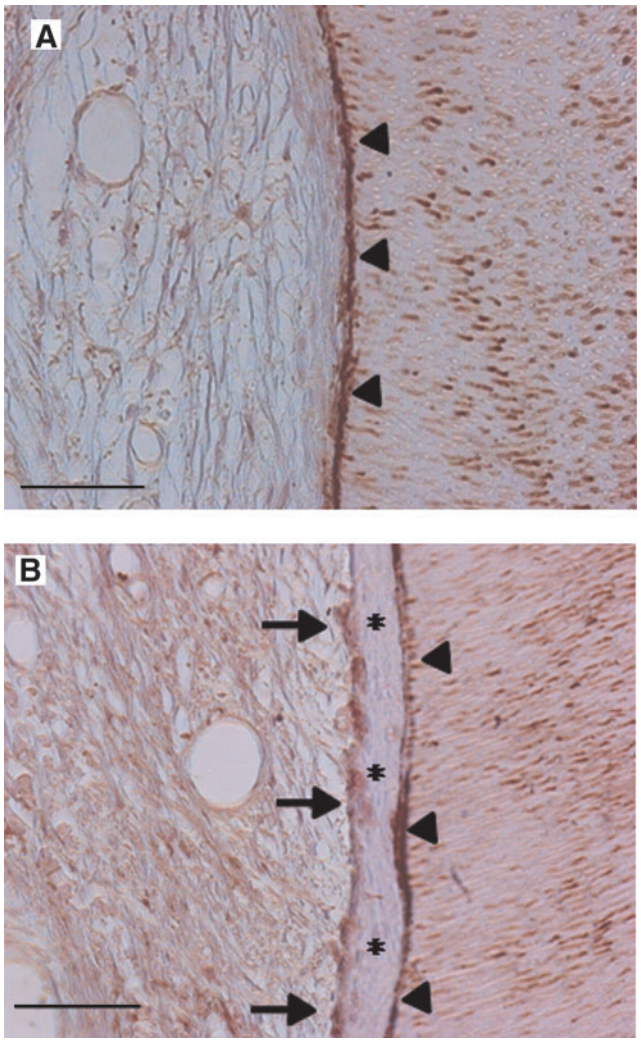

FIG. 8. Immunolocalization of OPN. **(A)** Magnification of the rectangular area shown in Figure 5B(b). **(B)** Magnification of the rectangular area shown in Figure 5D(c). The dentin surface (arrowheads) and cementoblasts (arrows) were immunoreactive for OPN. *New cementum. Bars: 50 μm.

The BDNF release profile from HMW-HA, as measured by ELISA, demonstrated that HMW-HA has the ability to retain BDNF and to release low levels of BDNF in a sustained manner for 2 weeks. The sustained release of BDNF may be due to the electrostatic interaction of the basic amine-rich N-terminus of BDNF with the acidic carboxylic acid residues of HA inducing tighter binding between BDNF and HMW-HA. Previous studies have shown that controlled release of cytokines is effective for tissue regeneration.[38,39] HMW-HA degradation may be accelerated by hyaluronidases *in vivo*. Therefore, HMW-HA, which is able to sustainedly release BDNF, is an effective scaffold for the induction of periodontal tissue regeneration.

CD44 is expressed by many cell types including, leukocytes, fibroblasts, epithelial cells, keratinocytes, endothelial cells, osteoclasts, and osteocytes.[40–43] In the present *in vivo* study, the early phase of periodontal tissue regeneration involved CD44-immunoreactive cells. This suggests that CD44

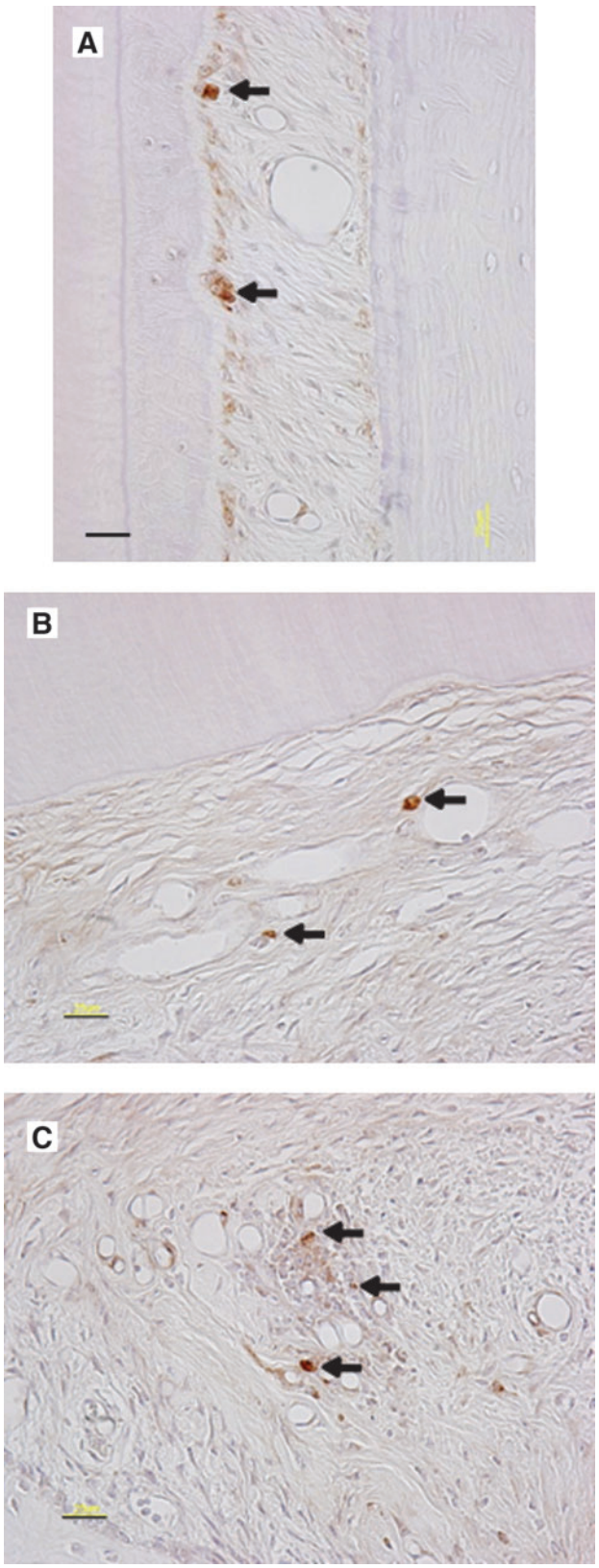

FIG. 9. Immunolocalization of protein gene protein 9.5. **(A)** Magnification of the rectangular area shown in Figure 5D(d). **(B)** Magnification of the rectangular area shown in Figure 5D(e). **(C)** Magnification of the rectangular area shown in Figure 5D(f). Arrows: protein gene protein 9.5-immunoreactive cells. Bars: 20 μm.

plays a role in HMW-HA-mediated events during periodontal tissue regeneration. In addition, CD44-immunoreactive cells on the dentin surface may possess potential for the formation of cementum and the periodontal ligament.

The present *in vivo* study showed that fewer inflammatory cells infiltrated into the defects in the HMW-HA group than in the sham operation group although no statistically significant difference in the amount or length of newly formed alveolar bone and cementum, respectively, was observed between the two groups. HMW-HA has an anti-inflammatory effect[24] and so may suppress inflammatory cell infiltration. In a previous study, BDNF/atelocollagen complex enhanced periodontal tissue regeneration in experimental class III furcation defects.[5] In the present study, BDNF/HMW-HA complex also enhanced periodontal tissue regeneration without epithelial cell invasion and with less inflammation, suggesting that HMW-HA as well as atelocollagen can maintain the regenerative activity of BDNF. HMW-HA may assist the regenerative activity of BDNF via stimulatory effects on the adhesion and proliferation of HPL cells.

PLGA is attracting great interest in the area of biomedical sciences. PLGA is mainly used as a medicine carrier that allows controlled release *in vivo* or on a cell-specific basis to restore soft tissue defects.[44] However, in the present study, the PLGA group and the BDNF/PLGA group did not enhance periodontal tissue regeneration compared to the HMW-HA group and the BDNF/HMW-HA group, respectively. The inflammatory cell infiltration was observed in the PLGA group and the BDNF/PLGA group. During the degradation of PLGA, there is minimal systemic toxicity, although in some cases, its acidic degradation products decrease the pH in the surrounding tissue, which results in local inflammatory reaction and poor tissue regeneration.[45,46] The decrease of the pH in the surrounding tissue accompanied by the degradation of PLGA may impair the BDNF-induced periodontal tissue regeneration. Further, the impaired periodontal tissue regeneration by PLGA suggests that not every scaffold can maintain the activity of BDNF for periodontal tissue regeneration.

The regeneration of cementum is thought to be critical for the establishment of a functional periodontal ligament.[11] The accumulation of OPN on the denuded dentin surface is the primary event that occurs during cementum regeneration.[47] In the HMW-HA group, OPN was immunolocalized on the denuded dentin surface, whereas no new cementum was generated. In the BDNF/HMW-HA group, OPN was immunolocalized on the cementoblasts lining the cementum surface and on the interface between the dentin and cementum. These findings indicated that the newly formed thin tissues along the root surface were new cementum. The difference in cementum formation between the two groups may have resulted from the ability of BDNF to stimulate the expression of bone (cementum)-related proteins, such as ALP, OPN, OCN, and BMP-2 in cultured HPL cells,[5] whereas HMW-HA does not have a stimulatory effect on bone (cementum)-related protein expressions. Although it is unclear from the present data why OPN was detected on the dentin surface of HMW-HA group, contrary to the non-stimulatory effect of HMW-HA on OPN expression in cultures of HPL cells, the anti-inflammatory and cell adhesion effects of HMW-HA may be involved in OPN accumulation on the denuded dentin surface.

The periodontal ligament functions as a sensory apparatus as well as a tooth supporting and anchoring tissue.[48] Stimulation of the teeth evokes various oral reflexes via the periodontal mechanoreceptors. The periodontal ligament contains two types of sensory receptors: free and specialized nerve terminals. The former, which are distributed extensively in the periodontal ligament, are mainly nociceptor, whereas the latter are mechanoreceptors involved in the control of mastication.[48] Our immunohistochemical study of PGP 9.5, a marker of neurons, has shown that the regenerated periodontal tissue promoted by BDNF/HA complex contains PGP 9.5-immunoreactive cells, whereas no nerve fibers were stained with anti-PGP 9.5 antibody. This suggests that the regenerated periodontal tissue induced by BDNF/HMW-HA complex functions as a sensory apparatus as well as a tooth supporting and anchoring tissue. PGP 9.5 is also expressed in hepatic stem cells, beta-cells, and pancreatic endocrine progenitor cells.[49,50] Further studies are necessary to confirm which types of cells express PGP 9.5 in periodontal tissue.

In conclusion, although HMW-HA alone does not markably enhance periodontal tissue regeneration, HMW-HA can assist BDNF activity in regenerating periodontal tissue, suggesting HMW-HA is an adequate scaffold for the clinical application of BDNF.

Acknowledgments

This work was supported in part by a Grant-in-Aid for Scientific Research (B) (No. 21390557) and a Grant-in-Aid for the Encouragement of Young Scientists (B) (No. 20791466) from the Japan Society for the Promotion of Science, Japan. The authors thank TWO CELLS. Co., Ltd., and in particular, Koichiro Tsuji, their President and Chief Executive Officer, for his insightful review of the article. We also thank the Analysis Center of Life Science of Hiroshima University and the Committee of Research Facilities for Laboratory Animal Science of Hiroshima University, for the use of their facilities.

Disclosure Statement

No competing financial interests exist.

References

1. Johnson, D., Lanahan, A., Buck, C.R., Sehagal, A., Morgan, C., Mercer, E., Bothwell, M., and Chao, M. Expression and structure of the human NGF receptor. Cell **47,** 545, 1986.
2. Radeke, M.J., Misko, T.P., Hsu, C., Herzenberg, L.A., and Shooter, E.M. Gene transfer and molecular cloning of the rat nerve growth factor receptor. Nature **325,** 593, 1987.
3. Barbacid, M. The Trk family of neurotrophin receptors. J Neurobiol **25,** 1386, 1994.
4. Ebendal, T. Function and evolution in the NGF family and its receptors. J Neurosci Res **32,** 461, 1992.
5. Takeda, K., Shiba, H., Mizuno, N., Hasegawa, N., Mouri, Y., Hirachi, A., Yoshino, H., Kawaguchi, H., and Kurihara, H. Brain-derived neurotrophic factor enhances periodontal tissue regeneration. Tissue Eng **11,** 1618, 2005.
6. Kajiya, M., Shiba, H., Fujita, T., Ouhara, K., Takeda, K., Mizuno, N., Kawaguchi, H., Kitagawa, M., Takata, T., Tsuji, K., and Kurihara, H. Brain-derived neurotrophic factor stimulates bone/cementum-related protein gene expression in cementoblasts. J Biol Chem **283,** 16259, 2008.

7. Kajiya, M., Shiba, H., Fujita, T., Takeda, K., Uchida, Y., Kawaguchi, H., Kitagawa, M., Takata, T., and Kurihara, H. Brain-derived neurotrophic factor protects cementoblasts from serum starvation-induced cell death. J Cell Physiol **221,** 696, 2009.
8. Nakahashi, T., Fujimura, H., Altar, C.A., Li, J., Kambayashi, J., Tandon, N.N., and Sun, B. Vascular endothelial cells synthesize and secrete brain-derived neurotrophic factor. FEBS Lett **470,** 113, 2000.
9. Nakanishi, T., Takahashi, K., Aoki, C., Nishikawa, K., Hattori, T., and Taniguchi, S. Expressions of nerve growth factor family neurotrophins in a mouse osteoblastic cell line. Biochem Biophys Res Commun **198,** 891, 1994.
10. Kerschensteiner, M., Gallmeier, E., Behrens, L., Leal, V.V., Misgeld, T., Klinkert, W.E., Kolbeck, R., Hoppe, E., Oropeza-Wekerle, R.L., Bartke, I., Stadelmann, C., Lassmann, H., Wekerle, H., and Hohlfeld, R. Activated human T cells, B cells, and monocytes produce brain-derived neurotrophic factor *in vitro* and in inflammatory brain lesions: a neuroprotective role of inflammation? J Exp Med **189,** 865, 1999.
11. Somerman, M.J., Ouyang, H.J., Berry, J.E., Saygin, N.E., Strayhorn, C.L., D'Errico, J.A., Hullinger, T., and Giannobile, W.V. Evolution of periodontal regeneration: from the roots' point of view. J Periodontal Res **34,** 420, 1999.
12. Somerman, M.J., Young, M.F., Foster, R.A., Moehring, J.M., Imm, G., and Sauk, J.J. Characteristics of human periodontal ligament cells *in vitro*. Arch Oral Biol **35,** 241, 1990.
13. McCulloch, C.A.G., and Bordin, S. Role of fibroblast subpopulations in periodontal physiology and pathology. J Periodontal Res **26,** 144, 1991.
14. Nohutcu, R.M., McCauley, L.K., Koh, A.J., and Somerman, M.J. Expression of extracellular matrix proteins in human periodontal ligament cells during mineralization *in vitro*. J Periodontal **68,** 320, 1997.
15. Taba, M., Jr., Jin, Q., Sugai, J.V., and Giannobile, W.V. Current concepts in periodontal bioengineering. Orthod Craniofac Res **8,** 292, 2005.
16. Hardingham, T.E., and Fosang, A.J. Proteoglycans: many forms and many functions. FASEB J **6,** 861, 1992.
17. Chen, W.Y., and Abatangelo, G. Functions of hyaluronan in wound repair. Wound Repair Regen **7,** 79, 1999.
18. Goa, K.L., and Benfield, P. Hyaluronic acid. A review of its pharmacology and use as a surgical aid in ophthalmology, and its therapeutic potential in joint disease and wound healing. Drugs **47,** 536, 1994.
19. Weigel, P.H., Fuller, G.M., and Le Boeuf, R.D. A model for the role of hyaluronic acid and fibrin in the early events during the inflammatory response and wound healing. J Theor Biol **119,** 219, 1986.
20. Weigel, P.H., Hascall, V.C., and Tammi, M. Hyaluronan synthases. J Biol Chem **272,** 13997, 1997.
21. Toole, B.P. Hyaluronan: from extracellular glue to pericellular cue. Nat Rev Cancer **4,** 528, 2004.
22. Noble, P.W. Hyaluronan and its catabolic products in tissue injury and repair. Matrix Biol **21,** 25, 2002.
23. David-Raoudi, M., Tranchepain, F., Deschrevel, B., Vincent, J.C., Bogdanowicz, P., Boumediene, K., and Pujol, J.P. Differential effects of hyaluronan and its fragments on fibroblasts: relation to wound healing. Wound Repair Regen **16,** 274, 2008.
24. Kato, Y., Nakamura, S., and Nishimura, M. Beneficial actions of hyaluronan (HA) on arthritic joints: effects of molecular weight of HA on elasticity of cartilage matrix. Biorheology **43,** 347, 2006.
25. Mitsui, Y., Gotoh, M., Nakama, K., Yamada, T., Higuchi, F., and Nagata, K. Hyaluronic acid inhibits mRNA expression of proinflammatory cytokines and cyclooxygenase-2/prostaglandin E(2) production via CD44 in interleukin-1-stimulated subacromial synovial fibroblasts from patients with rotator cuff disease. J Orthop Res **26,** 1032, 2008.
26. Aruffo, A., Stamenkovic, I., Melnick, M., Underhill, C.B., and Seed, B. CD44 is the principal cell surface receptor for hyaluronate. Cell **61,** 1303, 1990.
27. Laurent, T.C., and Fraser, J.R. Hyaluronan. FASEB J **6,** 2397, 1992.
28. Chen, W.Y., and Abatangelo, G. Functions of hyaluronan in wound repair. Wound Repair Regen **7,** 79, 1999.
29. Puré, E., and Cuff, C.A. A crucial role for CD44 in inflammation. Trends Mol Med **7,** 213, 2001.
30. Ponta, H., Sherman, L., and Herrlich, P.A. CD44: from adhesion molecules to signalling regulators. Nat Rev Mol Cell Biol **4,** 33, 2003.
31. Polimeni, G., Xiropaidis, A.V., and Wikesjö, U.M. Biology and principles of periodontal wound healing/regeneration. Periodontol 2000 **41,** 30, 2006.
32. Pasquinelli, G., Orrico, C., Foroni, L., Bonafè, F., Carboni, M., Guarnieri, C., Raimondo, S., Penna, C., Geuna, S., Pagliaro, P., Freyrie, A., Stella, A., Caldarera, C.M., and Muscari, C. Mesenchymal stem cell interaction with a non-woven hyaluronan-based scaffold suitable for tissue repair. J Anat **213,** 520, 2008.
33. West, D.C., and Kumar, S. The effect of hyaluronate and its oligosaccharides on endothelial cell proliferation and monolayer integrity. Exp Cell Res **183,** 179, 1989.
34. Mast, B.A., Diegelmann, R.F., Krummel, T.M., and Cohen, I.K. Hyaluronic acid modulates proliferation, collagen and protein synthesis of cultured fetal fibroblasts. Matrix **13,** 441, 1993.
35. Bodo, M., Pezzetti, F., Baroni, T., Carinci, F., Arena, N., Nicoletti, I., and Becchetti, E. Hyaluronic acid modulates growth, morphology and cytoskeleton in embryonic chick skin fibroblasts. Int J Dev Biol **37,** 349, 1993.
36. Hehenberger, K., Kratz, G., Hansson, A., and Brismar, K. Fibroblasts derived from human chronic diabetic wounds have a decreased proliferation rate, which is recovered by the addition of heparin. J Dermatol Sci **16,** 144, 1998.
37. Moon, S.O., Lee, J.H., and Kim, T.J. Changes in the expression of cmyc, RB and tyrosine-phosphorylated proteins during proliferation of NIH 3T3 cells induced by hyaluronic acid. Exp Mol Med **30,** 29, 1998.
38. Wang, C.K., Ho, M.L., Wang, G.J., Chang, J.K., Chen, C.H., Fu, Y.C., and Fu, H.H. Controlled-release of rhBMP-2 carriers in the regeneration of osteonecrotic bone. Biomaterials **30,** 4178, 2009.
39. Lu, H.H., Vo, J.M., Chin, H.S., Lin, J., Cozin, M., Tsay, R., Eisig, S., and Landesberg, R. Controlled delivery of platelet-rich plasma-derived growth factors for bone formation. J Biomed Mater Res A **86,** 1128, 2008.
40. Lesley, J., Schulte, R., and Hyman, R. Binding of hyaluronic acid to lymphoid cell lines is inhibited by monoclonal antibodies against Pgp-1. Exp Cell Res **187,** 224, 1990.
41. Miyake, K., Underhill, C.B., Lesley, J., and Kincade, P.W. Hyaluronate can function as a cell adhesion molecule and CD44 participates in hyaluronate recognition. J Exp Med **172,** 69, 1990.
42. Lee, J.Y., and Spicer, A.P. Hyaluronan: a multifunctional, megaDalton, stealth molecule. Curr Opin Cell Biol **12,** 581, 2000.

43. Nakamura, H., Kenmotsu, S., Sakai, H., and Ozawa, H. Localization of CD44, the hyaluronate receptor, on the plasma membrane of osteocytes and osteoclasts in rat tibiae. Cell Tissue Res **280,** 225, 1995.
44. Cieślik, M., Mertas, A., Morawska-Chochól, A., Sabat, D., Orlicki, R., Owczarek, A., Król, W., and Cieślik, T. The evaluation of the possibilities of using PLGA co-polymer and its composites with carbon fibers or hydroxyapatite in the bone tissue regeneration process—*in vitro* and *in vivo* examinations. Int J Mol Sci **10,** 3224, 2009.
45. Taylor, M.S., Daniels, A.U., Andriano, K.P., and Heller, J. Six bioabsorbable polymers: *in vitro* acute toxicity of accumulated degradation products. J Appl Biomater **5,** 151, 1994.
46. Klompmaker, J., Jansen, H.W., Veth, R.P., de Groot, J.H., Nijenhuis, A.J., and Pennings, A.J. Porous polymer implant for repair of meniscal lesions: a preliminary study in dogs. Biomaterials **12,** 810, 1991.
47. Kawaguchi, H., Ogawa, T., Kurihara, H., and Nanci, A. Immunodetection of noncollagenous matrix proteins during periodontal tissue regeneration. J Periodontal Res **36,** 205, 2001.
48. Nandasena, B.G., Suzuki, A., Aita, M., Kawano, Y., Nozawa-Inoue, K., and Maeda, T. Immunolocalization of aquaporin-1 in the mechanoreceptive Ruffini endings in the periodontal ligament. Brain Res **1157,** 32, 2007.
49. Yamada, S., Terada, K., Ueno, Y., Sugiyama, T., Seno, M., and Kojima, I. Differentiation of adult hepatic stem-like cells into pancreatic endocrine cells. Cell Transplant **14,** 647, 2005.
50. Yokoyama-Hayashi, K., Takahashi, T., Kakita, A., and Yamashina, S. Expression of PGP9.5 in ductal cells of the rat pancreas during development and regeneration: can it be a marker for pancreatic progenitor cells? Endocr J **49,** 61, 2002.

Address correspondence to:
Katsuhiro Takeda, D.D.S., Ph.D.
Department of Periodontal Medicine
Division of Frontier Medical Science
Hiroshima University Graduate School of Biomedical Sciences
1-2-3, Kasumi, Minami-ku
Hiroshima 734-8553
Japan

E-mail: takepon@hiroshima-u.ac.jp

Received: February 5, 2010
Accepted: November 22, 2010
Online Publication Date: December 28, 2010